J1.1 LARGE-SCALE ATMOSPHERE-OCEAN-LAND INTERACTION IN THE FORMATION OF SUMMERTIME SUBTROPICAL HIGHS

Hisashi Nakamura* and Takafumi Miyasaka
Department of Earth and Planetary Science, University of Tokyo, Tokyo, JAPAN

1. INTRODUCTION

Subtropical highs reside over the eastern portions of ocean basins throughout the year. In the Northern Hemisphere (NH), they tend to be stronger in summer than in winter, especially over the North Pacific. A surface subtropical high drives a subtropical oceanic gyre, forming a cool equatorward current off the west coast of a continent to the east. The strong surface northerlies along the eastern flank of the high act to maintain cool sea-surface temperatures (SSTs) underneath by enhancing coastal upwelling and evaporation. The presence of the cool SSTs and a mid-tropospheric subsidence favors the local development of marine stratus in the planetary boundary layer (PBL). Their high albedo also acts to maintain the cool SSTs.

It is still unsolved how the subtropical anticyclone cells in the NH summer are forced and maintained. A theory of a zonally-sym-metric Hadley circulation predicts much weaker subsidence in the summer hemisphere than in the winter hemisphere, which is thus unfavorable for the maintenance of the summertime subtropical highs. Moreover, as shown below, the observed summertime subtropical highs are in the form of high-pressure cells, suggesting that dynamics of the highs may be better understood in the context of planetary waves. Hoskins and Rodwell (1995) reproduced the summertime planetary waves and associated surface subtropical highs in a time-dependent nonlinear primitive equation (PE) model with the observed diabatic heating pattern. To substantiate a hypothesis proposed by Hoskins (1996), Rodwell and Hoskins (2001) further examined the dynamics of the individual summertime subtropical highs over the whole globe as a nonlinear PE model response to regional diabatic heating with realistic topography. They concluded that the combined effect of the topography and monsoonal heating to the east (i.e., the North American monsoon for the North Pacific high and the Asian monsoon for the Azores high) is of primary importance for the generation of the surface subtropical highs and subsidence aloft, in addition to the effect of the local cooling over the eastern oceans. They thus emphasized the upstream influence of the monsoonal heating on the formation of a summertime subtropical high, which was argued against by Chen et al. (2001), who claimed by using a linearized quasi-geostrophic model that each of the summertime NH subtropical highs is maintained as a component of stationary baroclinic Rossby waves forced by upstream monsoonal heating. However, the modeling by Chen et al. (2001) is too idealized to explain the distinct vertical structure of the observed summertime planetary waves (i.e., baroclinic and equivalent barotropic structures in the subtropics and midlatitudes, respectively). Furthermore, deep structure of the diabatic heating assigned in their model both for the continental heating and maritime cooling is also far from reality. As Wu and Liu (2003) demonstrated, both heating over the western portion of a subtropical continent and maritime cooling off the west coast of the continent are confined to the lower troposphere. Hence, the model experiment by Rodwell and Hoskins (2001) is likely more plausible than the idealized model experiment by Chen et al. (2001). In fact, Liu et al. (2004) showed that the zonal heating contrast can force the surface subtropical highs. Seager et al. (2003) showed through numerical experiments with AGCMs coupled with an oceanic mixed layer model that the coolness of the eastern subtropical ocean is more important in forcing the summertime subtropical anticyclones, emphasizing the particular importance of local air-sea interaction.

No specific assessment, however, has been made in the aforementioned studies about the relative importance of the deep convective heating and the shallow cooling associated with maritime stratus. Another important issue is to clarify the dynamical characteristics of the three-dimensional structure of the summertime subtropical highs and the associated planetary waves. An issue of particular interest is how much contribution can be made by the shallow, lower-tropospheric heating/cooling couplets across the west coasts of North America and North Africa to the generation of the observed upper-level planetary waves and associated near-surface circulation including the subtropical highs. Despite the interactive nature between surface subtropical anticyclones and associated lower-tropospheric cooling (Hoskins 1996; Rodwell and Hoskins 2001; Seager et al. 2003), it is nevertheless informative to confirm that part of the feedback loop is indeed operative as the atmospheric response to the prescribed near-surface diabatic heating.

The present study is conducted to examine the dynamical and thermodynamical issues addressed above in relation to the subtropical anticyclones observed in the NH summer. Our study suggests that, although the monsoon-desert mechanism argued in

* *Corresponding author address:* Hisashi Nakamura, Dept. of Earth & Planetary Science, Univ. of Tokyo, Tokyo, 113-0033, JAPAN; e-mail: hisashi@eps.s.u-tokyo.ac.jp

Hoskins (1996) and Rodwell and Hoskins (2001) may be important in maintaining the dryness of the western portion of the continents, the summertime subtropical highs should essentially be interpreted in the framework of local atmosphere-ocean-land interactions. Details are found in Miyasaka and Nakamura (2004).

2. DATA AND ATMOSPHERIC MODEL

In this study, we use monthly-mean global circulation data based on the National Centers for Environmental Prediction/National Center for Atmospheric Research (NCEP/NCAR) reanalyses from 1979 to 1998. Since the particular reanalysis scheme is known to contain some problems in diabatic heating fields (Kalnay et al. 1996), we use monthly-mean fields of diabatic heating obtained from the NCEP/ Department of Energy (DOE) Atmospheric Model Intercomparison Project (AMIP-II) reanalyses from 1979 to 1993 (Kanamitsu et al. 2002), in which radiation processes have been improved.

Vertical motion associated with vorticity and heat transport by planetary waves can be diagnosed with an omega equation linearized about the climatological-mean zonally-uniform flow for July. In recognition of the fact that warm and cold anomalies at the surface are equivalent to cyclonic and anticyclonic potential-vorticity (PV) anomalies, respectively, the influence of zonally-asymmetric surface potential temperature (θ^*) upon the tropospheric circulation, the PV inversion technique is utilized (Hoskins et al. 1985).

The model used in this study is a global nonlinear PE model with simplified physical processes. It was originally developed at Reading University and has been modified for the study of the summertime planetary waves. To resolve shallow diabatic heating confined mainly into PBL, the model vertical resolution has been set twice as high as in Rodwell and Hoskins (2001). The zonal-mean state was fixed throughout an integration. Since it takes 10~15 days for surface subtropical highs to develop in the model after diabatic heating has been switched on, we will show 10-day average fields from the 16-th to 25-th day of our integrations. In experiments with topography, the surface elevation had been raised gradually over a 5-day period before diabatic heating was imposed.

In a set of our experiments, horizontal distribution of the zonally asymmetric component of diabatic heating measured as the rate of a local temperature change was taken from the AMIP-II reanalysis data at each of the 27 σ-levels of the reanalysis system and then interpolated onto equally spaced model σ-levels. In another set of experiments, the near-surface diabatic heating field was determined by relaxing the zonally-asymmetric component of the model temperatures below the level of $\sigma = 0.677$ toward the corresponding observational values taken from the NCEP/NCAR reanalyses. This particular set of experiments was performed without the land-surface elevation. The relaxation time of 0.5 day was found necessary for attaining diabatic heating with magnitude comparable to that of the corresponding heating obtained from the AMIP-II reanalysis data. In each set of those experiments, diabatic heating was assigned (or evaluated) with its full intensity within a rectangular domain (or latitudinal band). Outside of the domain, the intensity of the heating was reduced linearly with latitude or longitude in such a way that it vanishes 10° in latitude or longitude away from the domain boundaries.

3. OBSERVATIONS

a. Three-dimensional structure

Each of the summertime subtropical highs in the climatological-mean NH sea-level pressure (SLP) field is in a cell-type configuration. Their centers positioned at ~35°N are shifted to the eastern portions of the basins (Fig. 1a). Thus, the highs accompany strong along-shore winds that advect the positive planetary vorticity. As argued previously (Hoskins 1996; Rodwell and Hoskins 2001; Seager et al. 2003), this low-level *ß* effect is balanced with the vorticity-tube shrinking associated with a strong subsidence off the coasts (Fig. 1b). The upper-level convergence associated with that subsidence yields cyclonic vorticity tendency, which is canceled mainly by the zonal advection of anticyclonic vorticity. This advection occurs to the east of upper-level anticyclonic vorticity that constitutes a meridional dipole with cyclonic vorticity to its south (Fig. 2b). As the node line of the dipole exhibits a SW-NE tilt, the mid-tropospheric descent spreads southwestward from its maximum (Fig. 1b), covering most of the area of the surface anticyclone to maintain it against the surface friction. Anticyclonic planetary vorticity advection along the eastern fringe of the upper-tropospheric cyclonic anomalies also acts to offset the effect of the subsidence at subtropical latitudes.

The association of the surface subtropical highs with the meridional vorticity dipoles aloft is a manifestation of baroclinic and equivalent barotropic structures in the southern and northern portions of the surface anticyclones, respectively, as observed by White (1982). The dipole structure is also hinted in the zonally asymmetric component of upper-tropospheric geopotential height as particularly deep pressure troughs above the southern portions of the surface subtropical highs. In a manner consistent with the upper-level dipoles, double-jet structures are evident above the surface subtropical highs (Fig. 1c), with the exits of midlatitude westerly jets to the north of the dipoles and the entrances of subtropical westerly jets to their south. Coriolis force acting on equatorward and poleward ageostrophic winds at the exits and entrances of the jets, respectively, is balanced mainly with the zonal westerly momentum advection. Thus, the upper-level convergence over the surface subtropical highs is dynamically consistent. In fact, the vertical motion diagnosed with the linearized omega equation to which

the heat and vorticity transport associated with the observed planetary waves was given can account for ~60% of the observational subsidence above the Pacific subtropical high and ~75% of the observed descent above the Azores High (Figs. 1b and 2a). This result indicates that the surface subtropical highs over the summertime NH can be regarded as part of the tropospheric planetary waves.

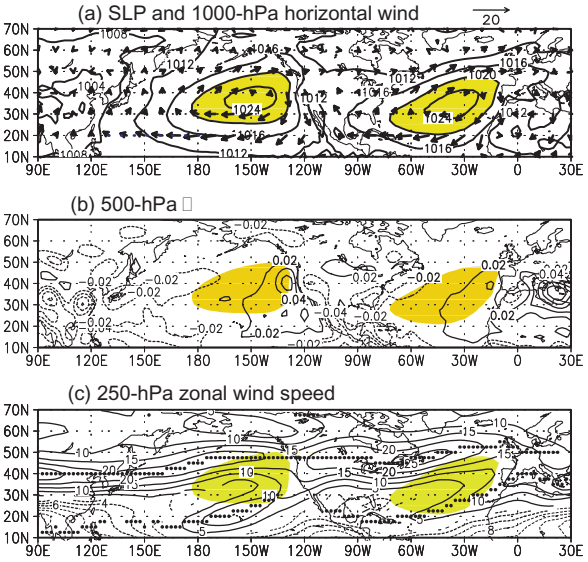

Figure 1: July climatologies of (a) SLP (every 4 hPa) and 1000-hPa horizontal wind (arrows), (b) 500-hPa *p*-velocity (every 0.02 Pa s^{-1}; solid lines for subsidence and dashed lines for uprising), and (c) 250-hPa horizontal wind speed (every 5 m s^{-1}; dashed lines for the easterlies). In (a), scaling for arrows (unit: m s^{-1}) is given at the top. In (a-c), shading is applied where SLP exceeds 1020 (hPa) and zero lines are omitted. In (c), local 250-hPa westerly jet axes are indicated with dots. Based on the NCEP/NCAR reanalyses.

b. Wave-activity propagation

The horizontal component of Plumb's (1985) wave-activity flux (***W***) associated with the upper-tropospheric climatological planetary waves observed in July exhibits no indication of an incoming wavetrain into the North Pacific subtropical high (Fig. 2b), as opposed to a numerical experiment by Chen et al. (2001). Rather, ***W*** diverges out of the vorticity dipole above of that high with the significant upward flux in the mid-troposphere (Fig. 2c), suggesting that the source of the planetary waves must be associated with the surface subtropical high. As in the North Pacific, the upward flux is evident also above the Azores high, although the upper-level wave-activity injection from upstream is stronger. Interestingly, it appears in Fig. 2b that wave activity generated around the North Pacific subtropical high propagates across North America into the North Atlantic, seemingly reinforcing the vorticity dipole above the Azores high. This wavetrain may be reinforced with the upward wave-activity injection near the Hudson Bay.

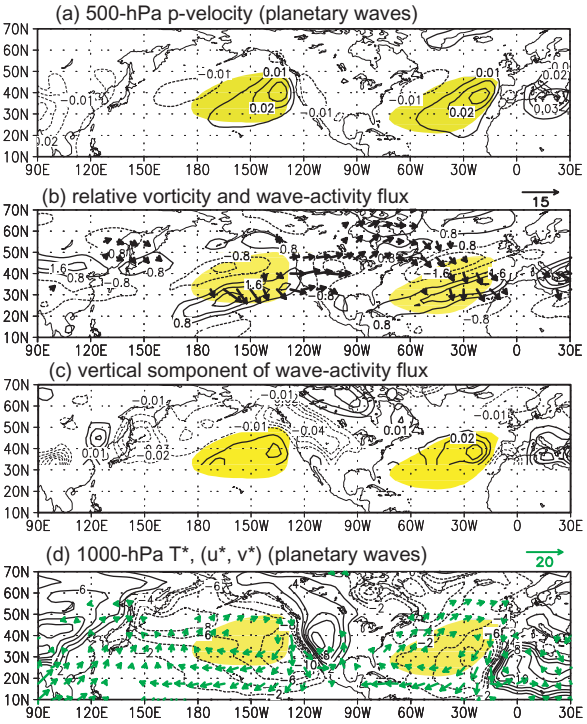

Figure 2: July climatologies of planetary waves based on zonally asymmetric fields of the NCEP/NCAR reanalyses. (a) 500-hPa *p*-velocity (every 0.01 Pa s^{-1}; solid and dashed lines for subsidence and uprising, respectively). (b) Horizontal component of Plumb's (1985) wave-activity flux (arrows) at the 250-hPa level, superimposed on 250-hPa relative vorticity associated with planetary waves (every 0.8 x10^{-5} s^{-1}; dashed for anticyclonic). Scaling (unit: m^2 s^{-2}) for arrows is given at the top. (c) Vertical component of the wave-activity flux (m^2 s^{-2}) at the 500-hPa level. Solid and dashed lines signify the upward and downward flux, respectively. (d) 1000-hPa horizontal wind (arrows) and temperature (contoured for every 2 K; dashed for negative values), both associated with planetary waves. In (a-d), shading is applied where the total SLP exceeds 1020 (hPa), and zero lines are omitted.

c. Diabatic heating and land-sea thermal contrasts

Among several types of diabatic heating known as important forcing of the summertime planetary waves, deep convective heating is rather weak to the east of each of the subtropical highs (Fig. 3b), as opposed to what is indicated in a schematic diagram proposed by Hoskins (1996). Rather, as Wu and Liu (2003) pointed out based on the NCEP/NCAR reanalyses, lower-tropospheric radiative cooling and sensible heating are dominant over the eastern portions of the subtropical ocean basins and over the western portions of the subtropical continents, respectively in the NCEP/DOE AMIP-II data set (Fig. 3b). The latter regions include (semi-) desert areas heated by strong summertime insolation. The shallow cooling is associated with persistent stratus clouds within the marine PBL developed over the cool California and Canary Currents (Klein and Hartmann 1993). In fact, in the summertime extratropical NH, the most pronounced surface thermal

contrasts are observed across the west coasts of the subtropical continents (Fig. 2d), just east of the Azores and Pacific subtropical highs. Low SSTs that contribute to these thermal contrasts are maintained through local air-sea interaction (Seager et al. 2003).

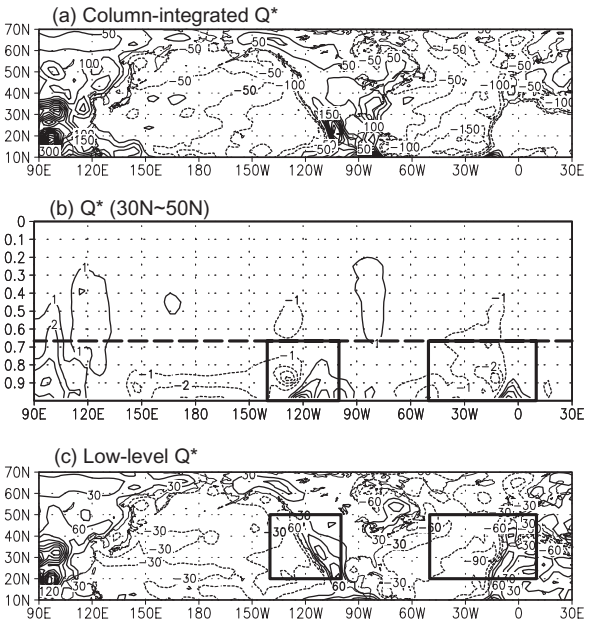

Figure 3: Zonally asymmetric component of climatological-mean diabatic heating (Q^*) for July obtained from the NCEP/DOE AMIP-II reanalysis data. (a) Column integrated heating (every 50 W m^{-2}). (b) Longitude-vertical section of Q^* as an average between 30° and 50°N (every 1 K/day). (c) Vertically integrated heating for $0.667 < \sigma < 1$ (every 30 W m^{-2}). In (a-c), dashed lines denote cooling and zero lines are omitted. In (b-c), rectangles signify the forcing domains for model simulations in subsections 4b and 4c. In (b), long-dashed lines signify the lower boundary of the upper-level forcing for experiment shown in Fig. 10.

Since surface temperature anomalies (θ^*) are equivalent to PV anomalies (Hoskins et al. 1985), the thermal contrasts in the summertime sub-tropics act to induce cyclonic and anticyclonic circulation over the heated land surface and the cool ocean surface, respectively, with northerly along-shore winds in between whose strength is proportional to the thermal contrast. This potential effect has been confirmed by applying the PV inversion with the observed 1000-hPa θ^* field. The induced winds decay upward at the rate of the Rossby depth. The induced northerlies advect cooler air and positive planetary vorticity, which can be balanced if the mid-tropospheric subsidence and associated near-surface divergence, respectively, are induced. In fact, a subsidence is evident to the east of each of the surface subtropical highs, in the field of vertical motion as diagnosed by substituting the wind and temperature fields obtained through the PV inversion into the omega equation linearized about the climatological zonal-mean state for July. The diagnosed subsidence is only about a quarter in strength compared to the observation, as the PV anomalies were assigned only at the surface. Furthermore, the diagnosed descent is shifted somewhat to the east of its observational counterpart, because the induced surface wind over the land surface was much stronger than in the real atmosphere due to the lack of surface friction in the PV inversion. In reality, the northerlies are strongest over the ocean where the friction is much weaker than over the land, and so is the subsidence. Nevertheless, our PV inversion and the subsequent diagnosis of the induced vertical motion have revealed the potential importance of the surface thermal contrast across the west coast of a subtropical continent for the formation of a summertime subtropical high.

4. MODEL SIMULATION

a. Remote influence

In this section, the reproducibility of the climatological-mean NH summertime planetary waves in the PE model described in section 2 is examined. In our first experiment, climatological-mean global diabatic heating for July based on the AMIP-II reanalyses at every vertical levels was used as the forcing with the global topography. Only the zonally asymmetric component of the heating (Q^*) was imposed as the forcing in the model in which the observed July climatology of the zonal-mean state was prescribed. In the SLP response, the subtropical high is well reproduced over the North Pacific, and so is the Azores high though its northward extension is somewhat overestimated when compared to the observation (Figs. 4a-b). In another experiment in which the prescribed Q^* is limited to a latitudinal band of 20~ 50°N (Fig. 4c), no significant reduction is found in the magnitude of either of the subtropical highs, indicating that remote influence from tropical convection, is only of secondary importance in the formation of the NH summertime subtropical highs.

The importance of the upstream or downstream influence of the diabatic heating in the subtropics is assessed by limiting the heating in the model to either of the ocean basins. In an experiment in which the diabatic heating is imposed only over the North Pacific basin (Fig. 4d), the North Pacific subtropical high is again well reproduced with respect to its intensity and location, although its northward extension is slightly overestimated. Unlike in the idealized experiment by Chen et al. (2001), no noticeable influence of diabatic heating associated with the Indian Monsoon reaches the core region of the North Pacific high. Over the North Atlantic (Fig. 4e), basin-wide diabatic heating including convective heating over the southeastern U.S. is strong enough to account for ~70% of the magnitude of the Azores high simulated in response to the global heating (Fig. 4b). This result indicates that, unlike the argument by Rodwell and Hoskins (2001), the Azores high in July forms without upstream influence from the Indian Monsoon. The overall results in

Fig. 4 strongly suggest that the NH subtropical highs in July form in response primarily to local diabatic heating/cooling and the remote influence from the tropics or Indian Monsoon is only of secondary importance.

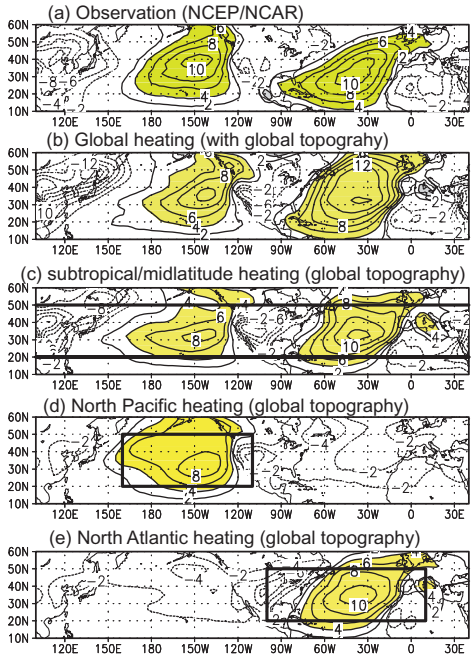

Figure 4: (a) Zonally-asymmetric climatological-mean SLP for July (every 2 hPa; dashed for negative values; zero contours omitted). As in (a), but for zonally-asymmetric SLP in the model with global topography. The model was forced with the climatological-mean global Q^* for July (see Fig. 3a) taken from the AMIP-II reanalyses. (c) As in (b), but for the model SLP response to Q^* given only in the latitudinal band of 20°~50°N. (d-e) As in (b), but for the model SLP response to Q^* given only in rectangular domains over (d) the North Pacific [20°~50°N, 160°E~110°W] and (e) the North Atlantic [20°~50°N, 100°W~10°E], respectively, as indicated.

b. Model simulation for the North Pacific

In order to substantiate the importance of the local land-sea thermal contrast in the formation of the NH subtropical highs in July, experiments were performed with the same model as used in section 4a but driven by diabatic heating prescribed only in relatively small regions. In the first experiment, we investigate the atmospheric response to Q^* prescribed in the Pacific/North American domain (Fig. 5a), which has been taken from the AMIP-II data set. Again, no topography is imposed ("no-mountain experiment"). In response to the thermal forcing, a surface temperature contrast across the California coast is again reproduced reasonably well (Fig. 5b). The subtropical high and surface along-shore wind are also reproduced reasonably well in the surface response, whose intensity reaches as much as ~70% of their observational counterpart (Figs. 2a and 5c). Though weaker than in the previous experiment and shifted slightly northward, a descent is also induced above the surface high as observed (Fig. 5c). Unlike in the observation, however, an ascent is noticeable to the south of the maritime descent. Despite this ascent acting to yield cyclonic circulation near the surface, the anticyclonic response dominates in the model SLP field. In the presence of this dipolar pattern in vertical motion, a stationary Rossby wave-train is generated in the upper troposphere propagating from the eastern Pacific to the North American continent (Fig. 5d), as indicated with the eastward wave-activity flux similar to the corresponding diagnosis for the observation (Figs. 2b and 5d). Unlike in the observation, however, the mid-tropospheric $\boldsymbol{W}$ is significantly upward south of 35°N only (Fig. 5d), and the wave activity generated in the subtropics is dispersed mainly poleward into the midlatitude westerlies. This southward shifted upward flux is in correspondence to the diabatic heating pattern of the AMIP-II reanalysis data, which is much stronger south of 35°N than to its north.

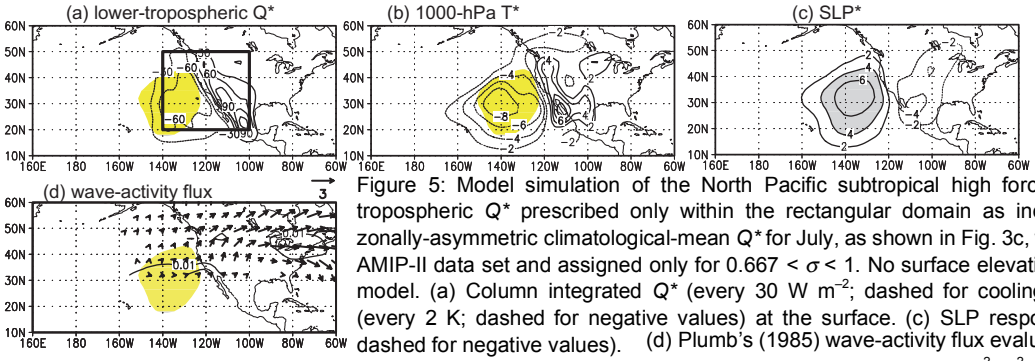

Figure 5: Model simulation of the North Pacific subtropical high forced with the lower-tropospheric Q^* prescribed only within the rectangular domain as indicated in (a). The zonally-asymmetric climatological-mean Q^* for July, as shown in Fig. 3c, was taken from the AMIP-II data set and assigned only for $0.667 < \sigma < 1$. No surface elevation is applied to the model. (a) Column integrated Q^* (every 30 W m^{-2}; dashed for cooling). (b) θ^* response (every 2 K; dashed for negative values) at the surface. (c) SLP response (every 2 hPa; dashed for negative values). (d) Plumb's (1985) wave-activity flux evaluated for the model response. Its horizontal component at the 250-hPa level is plotted with arrows whose scaling (unit: m^2 s^{-2}) is given below the panel. The upward component of the flux at the 500-hPa level is superimposed with solid lines (every 0.01 m^2 s^{-2}). In (a)-(d), shading is applied where the SLP response exceeds 4 (hPa).

In another experiment with global topography, cool temperature and anticyclonic anomalies both simulated over the eastern ocean (Figs. 6a-b) are somewhat weaker than in the no-mountain experiment (Figs. 5a-b), while the warm temperatures and cyclonic SLP anomalies over the continent are stronger. The inclusion of topography causes no significant changes in the strength of the land-sea thermal contrast (Fig. 6a) and thus in the associated SLP gradient (Fig. 6c) and along-shore surface wind (not shown). Rather, the presence of the Rockies acts to enhance the low-level heating and atmospheric response over the American continent. Since the diabatic heating as measured by the rate of air temperature change imposed at each of the σ levels is identical between the two experiments, the corresponding Q^* is larger over the elevated land surface than over the flat surface acting to enhance the low-level thermal response over the Rockies in the mountain experiment. Specifically, the near-surface warming is strongest near a Q^* maximum around Baja California in the no-mountain experiment, whereas in the mountain experiment, that is strongest over the U.S. Rockies, maximizing the land-sea thermal contrast at ~35°N. Thus, in the mountain experiment, the thermal forcing center for Rossby waves is closer to the zonal-mean westerly axis than in the no-mountain experiment, which renders the upward mid-tropospheric wave-activity flux stronger in the former experiment). The mid-tropospheric vertical motion is also enhanced locally. The meridional vorticity dipole in the upper troposphere above the surface high becomes doubled in strength due to the inclusion of topography (Fig. 6c). It is thus suggested that the Rocky mountains act to force the planetary waves not only through their mechanical effect but also through raising the heating altitude and shifting the effective thermal forcing poleward nearer to the mid-latitude westerlies jet, which leads to the stronger upper-level response.

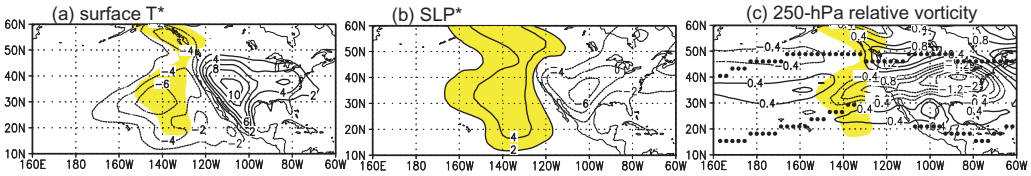

Figure 6: The same experiment as in Fig. 5, but with global topography. (a) θ^* response (every 2 K; dashed for negative values) at the surface. (b) Zonally-asymmetric SLP response (every 2 hPa; dashed for negative values). (c) Zonally-asymmetric response in 250-hPa relative vorticity (every 0.2 x10^{-5} s^{-1}; dashed for anticyclonic). The observed climatological-mean westerly jet axes are superimposed with dots. In (a)-(c), shading is applied where the SLP response exceeds 4 (hPa).

c. Model simulation for the North Atlantic

The same kind of numerical experiments as in the preceding subsection was performed with the atmospheric model forced by the lower-tropospheric heating/cooling contrast between the North Atlantic Ocean and the European and African continents (Fig. 7a). In this no-mountain experiment, the near-surface thermal contrast is well reproduced in intensity, in spite of somewhat overestimated maritime coolness and underestimated continental warmness (Fig. 7b). The strength of the surface subtropical high reaches ~75% of what is observed (Figs. 7c and 4a). A subsidence is evident in the eastern portion of the simulated Azores high, but it tends to be shifted poleward relative to its observational counterpart. As observed, the effect of the low-level divergence associated with the subsidence is balanced with the planetary vorticity advection by the northerlies along the eastern flank of the surface high. The center of the upper-level cyclonic vorticity response is located just *downstream* of the upper-level convergence associated with the subsidence, indicating the dominance of vorticity advection by the midlatitude westerlies. In reality, however, the effect of the upper-level convergence is balanced with the zonal advection of anticyclonic vorticity from *upstream*. Thus, the polarity of the vorticity dipole in the model is reversed with what is observed (Fig. 2b). Nevertheless, the model simulation suggests that the near-surface thermal contrast across the west coasts of North Africa and Europe bears the potential not only to force the surface Azores high but also to act as a source of upper-level planetary waves, as evident in the significant upward component of $\boldsymbol{W}$ and its upper-tropospheric divergence above the high (Fig. 7d).

The significance of the downstream influence of the North Pacific high and the Rockies upon the Azores high can be assessed in a model integration with realistic global topography and lower-tropospheric diabatic heating imposed only in the extratropical region extending eastward from the North Pacific to the North Atlantic across North America [20~50°N, 140°W~10°E]. No noticeable difference is found in the near surface thermal field over the North Atlantic, due to the inclusion of the Rockies and thermal forcing over the northeastern Pacific. Nevertheless, the upstream influence is significant in the upper troposphere, as a stationary Rossby wave packet forced over the eastern Pacific and the Rockies reaches into the North Atlantic, as observed. The packet appears to interfere with the locally forced Rossby waves over the Azores high, causing slight intensification of the surface Azores high.

Another factor that may contribute remotely to the enhancement of the surface Azores high is the deep

cumulus heating over the southeastern U.S. (Fig. 3). In the model SLP response to diabatic heating assigned only above the level of σ = 0.667, anticyclonic circulation is yielded reinforcing the surface Azores high, but it is substantially weaker than in the response to the local low-level heating contrast.

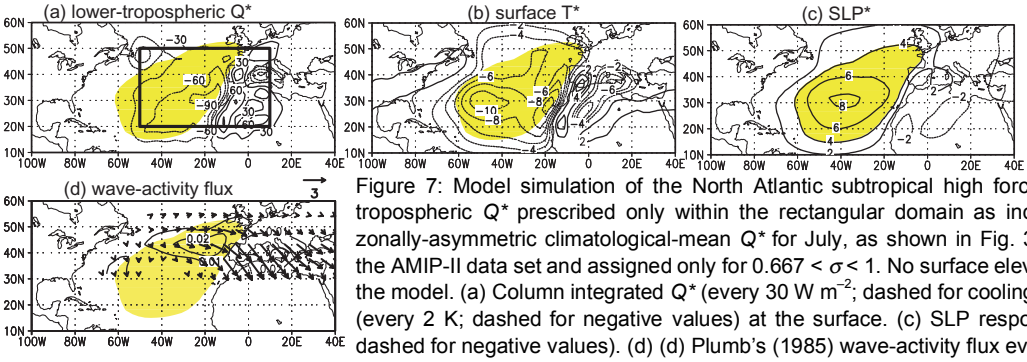

Figure 7: Model simulation of the North Atlantic subtropical high forced with the lower-tropospheric Q^* prescribed only within the rectangular domain as indicated in (a). The zonally-asymmetric climatological-mean Q^* for July, as shown in Fig. 3c, was taken from the AMIP-II data set and assigned only for $0.667 < \sigma < 1$. No surface elevation is applied to the model. (a) Column integrated Q^* (every 30 W m^{-2}; dashed for cooling). (b) θ^* response (every 2 K; dashed for negative values) at the surface. (c) SLP response (every 2 hPa; dashed for negative values). (d) (d) Plumb's (1985) wave-activity flux evaluated for the model response. Its horizontal component at the 250-hPa level is plotted with arrows whose scaling (unit: m^2 s^{-2}) is given below the panel. The upward component of the flux at the 500-hPa level is superimposed with solid lines (every 0.01 m^2 s^{-2}). In (a)-(d), shading is applied where the SLP response exceeds 4 (hPa).

d. Pre-monsoon season

The importance of the local land-sea thermal contrasts in the formation of subtropical highs can be further substantiated in similar numerical experiments performed for the pre-monsoon season. At this time of the year, the subtropical land-sea thermal contrasts become substantially strong in the presence of land-masses heated by insolation, whereas convective activity associated with the Indian and Mexican monsoon has not been fully matured yet (Figs. 3a and 8d). Specifically, land-sea thermal contrasts across the west coasts of the subtropical continents become as strong as 13~15°C in May (Fig. 8b), compared to 18~20°C in July (Fig. 1d). The cooling and heating maxima are shifted equatorward by ~5° relative to their July counterpart. Each of the subtropical highs observed in the North Pacific and the North Atlantic (i.e., the Azores high) displays a summertime characteristic of enhanced cross-shore SLP gradient in its eastern flank (Fig. 9a), though more elongated zonally than in July (Fig. 1a). The distribution of the lower-tropospheric Q^* (Fig. 8c) is in good correspondence with the observed distribution of the thermal contrast (Fig. 8b). Indeed, the total column heating around the west coasts of the subtropical continents is dominated by the low-level heating or cooling (Fig. 8d).

To assess the importance of the subtropical heating/cooling couplets for the formation of the subtropical highs in the pre-monsoon season, the same model simulations as in the previous subsections were repeated but with Q^* and the zonal mean state both fixed to their May climatologies. In the control run, in which Q^* at all vertical levels and the realistic topography were assigned globally, the subtropical highs can be well reproduced both over the North Pacific and North Atlantic (Fig. 9b). The simulated highs are somewhat overestimated when compared to their observational counterpart in the zonally asymmetric SLP field (Fig. 9a). In another simulation in which Q^* was imposed only in the lower troposphere over the North Pacific (Fig. 9c), the core region of the subtropical high can be reproduced well, whose strength reaches ~70% of that in the control run (Fig. 9b) and ~95% of its observational counterpart (Fig. 9a). The westward extension of the high is, however, seriously underestimated. In a companion experiment where the lower-

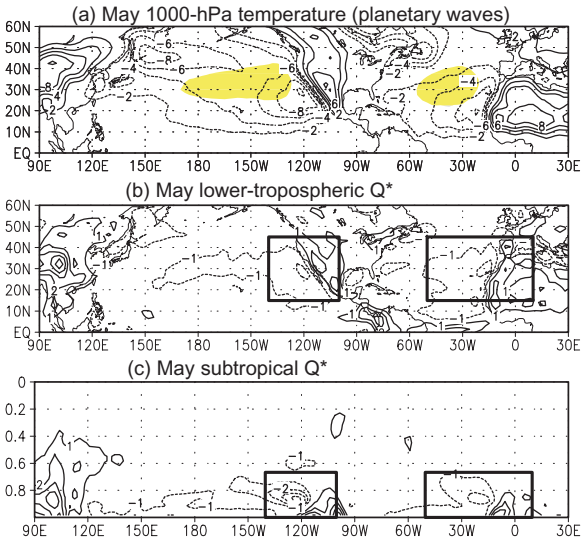

Figure 8: The May climatologies based on (a) the NCEP/NCAR and (b-c) the AMIP-II reanalyses. (a) Zonally asymmetric 1000-hPa temperature (every 2 K; dashed for negative value). (b) Zonally-asymmetric diabatic heating Q^* in the lower troposphere ($0.667 < \sigma < 1$) measured as the rate of temperature change (every 1 K day^{-1}). (c) Longitude-vertical section of Q^* as an average between 20 and 40°N (every 1 K day^{-1}). In (a), shading is applied where SLP exceeds 1020 (hPa). In (b-c), cooling is indicated with dashed lines, and rectangles signify forcing domains for model simulations.

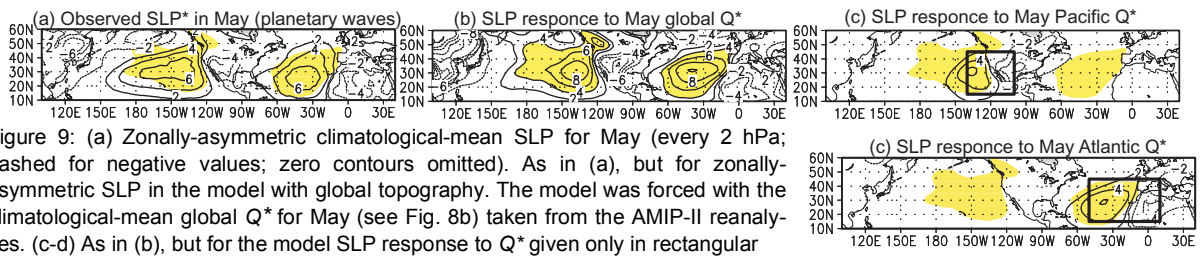

Figure 9: (a) Zonally-asymmetric climatological-mean SLP for May (every 2 hPa; dashed for negative values; zero contours omitted). As in (a), but for zonally-asymmetric SLP in the model with global topography. The model was forced with the climatological-mean global *Q** for May (see Fig. 8b) taken from the AMIP-II reanalyses. (c-d) As in (b), but for the model SLP response to *Q** given only in rectangular domains over (c) the North Pacific [15°~45°N, 140°~100°W] and (d) the North Atlantic [15°~45°N, 50°W~10°E], respectively, as indicated. In (a-d), shading is applied where the SLP response in (b) exceeds 4 (hPa).

tropospheric *Q** was assigned only over the North Atlantic (Fig. 9d), the strength of the Azores high reaches ~65% of that in the control run (Fig. 9b) and ~90% of its observational counterpart (Fig. 9a). These model experiments suggest that the local land-sea contrast can be the primary forcing factor for the core region of the subtropical high observed in May over each of the ocean basins, and the monsoonal heating may be only of secondary importance. Other factors that can act as significant forcing of the subtropical highs in May, particularly their westward extension, include feedback forcing from transient eddies migrating along the storm tracks located to the north of those highs.

5. Summary and Discussion

In this study, we have clarified the three-dimensional structure and formation dynamics of the climatological mean summertime subtropical highs observed in the NH. Those highs are accompanied locally by pronounced zonal contrasts in surface air temperature and near-surface diabatic heating across the west coasts of the subtropical continents. Using a nonlinear atmospheric model driven by a zonally-asymmetric diabatic heating pattern, we have shown the model SLP response only to a localized near-surface heating/cooling contrast as observed in July between the subtropical eastern North Pacific and western North America can account for ~70% of the observed strength of the Pacific high in July. This model response is understandable from a viewpoint of PV thinking, since cool and warm anomalies over the ocean and land surface act as anticyclonic and cyclonic PV anomalies, respectively, to yield strong equatorward along-shore winds. Vorticity and heat transport associated with the along-shore winds requires descent above the eastern portion of the subtropical high to maintain the vorticity and heat balance. This descent acts to maintain the surface anticyclone against the surface friction and also to generate upper-tropospheric planetary waves. Our diagnosis has revealed the strong upward component of the wave-activity flux of Rossby waves and its upper-level divergence above the surface subtropical highs over the eastern North Pacific and Atlantic, suggesting that the pronounced near-surface land-sea thermal contrasts accompanied by the subtropical highs can act as an important source of the summertime planetary waves over the western hemisphere. Essentially the same results have been obtained through our model experiments for those subtropical highs in May, when both of the Indian and Mexican monsoons have not been fully matured yet. We therefore conclude that, unlike the argument by Rodwell and Hoskins (2001), deep convective heating associated with the Indian and Mexican monsoons is only a secondary factor for the generation of the subtropical highs, as recently presented by Seager et al. (2003). Furthermore, we have found no significant downstream propagation of stationary Rossby waves into the Pacific subtropical high, unlike in the argument by Chen et al. (2001).

The land-sea thermal contrast involved in the formation of each of the subtropical highs is mainly a manifestation of the thermal effect of the low SSTs over the eastern ocean and radiative cooling associated with marine stratus and the heating effect through sensible heat flux over the landmass to the east. Seager et al. (2003) emphasized the importance of the thermal effect of the cool SSTs over the eastern oceans for the generation of the summertime subtropical highs. Wang et al. (2004) have demonstrated through their regional model experiment that radiative cooling off the Peruvian coast in austral spring enhances a surface subtropical anticyclone off the coast and the associated near-surface equatorward along-shore wind. The temperature inversion is associated with strong descent, low SSTs and cold advection by the along-shore equatorward winds, all of which would be augmented as the nearby subtropical high intensifies. The strong radiative cooling associated with the marine stratus, which has been shown in the present study to force the subtropical high, is thus maintained in the presence of the high, suggestive of a local feedback loop in the atmosphere-ocean-land system in the summertime subtropics (Ma et al. 1994). Owing to the heat capacity of landmasses much smaller than that of the ocean, this feedback loop must be triggered by landmass warming in late spring or early summer. In fact, our numerical experiment can reproduce the NH subtropical highs in May as a response to local low-level land-sea thermal contrasts in the presence of subtropical landmasses heated by insolation. The

presence of the feedback loop is suggested observationally in Fig. 10, in which changes in the climatological-mean evaporation over the NH from May to July are plotted on the basis of the NCEP/NCAR reanalysis data. The land-sea thermal contrast across the west coasts of the subtropical continents are enhanced (Fig. 10b), as the lower-tropospheric diabatic cooling in the extratropical eastern ocean is strengthened from spring to summer (Fig. 10a). Concomitantly, anticyclonic circulation at the surface intensifies over each of the ocean basins (Figs. 10b-c), accompanying the increasing northeasterly wind speed over the eastern portion of basin (Fig. 10d). The resultant increase in turbulent heat release from the ocean surface acts to retain cool SSTs locally and thereby contributes to the enhancement of the land-sea thermal contrast (Fig. 10b). These results support our hypothesis that the NH subtropical highs intensify from early to mid-summer periods through local feedback processes. Our numerical experiments suggest that the so-called monsoon-desert mechanism, as argued by Hoskins (1996) and later by Rodwell and Hoskins (2001), is only of a secondary factor for the formation of the observed summertime high-pressure cells in the NH subtropics. We conjecture, however, that the monsoon-desert mechanism contributes indirectly to the formation of the highs through maintaining the dryness of the western sectors of the subtropical continents (Chou et al. 2001) and thereby high surface temperature and associated near-surface sensible heating.

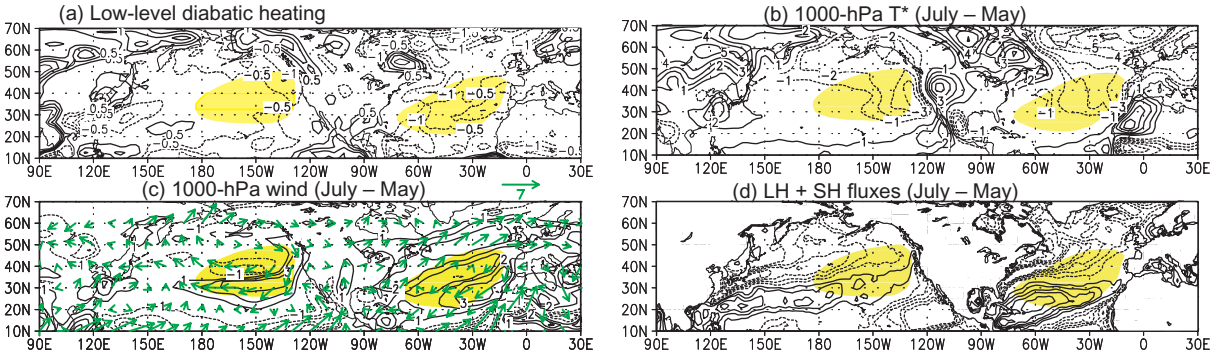

Figure 10: Difference maps between the July and May climatologies; (July minus May), based on the (a) AMIP-II and (b-d) NCEP/NCAR reanalyses. Shaded where the July SLP exceeds 1020 (hPa). (a) Zonally asymmetric diabatic heating in the lower troposphere ($0.667 < \sigma < 1$) measured as the rate of temperature change (every 0.5 K day^{-1}; dashed for cooling). (b) Zonally asymmetric 1000-hPa temperature (every 1 K; dashed for negative values). (c) 1000-hPa wind speed (contoured for every 1 m s^{-1}) and velocity (arrows). Scaling (unit: m s^{-1}) is at the top. (d) Surface turbulent heat flux (latent and sensible heat; contoured for every 10 W m^{-2}) over the ocean. Solid and dashed lines indicate enhanced and reduced heat release from the surface, respectively. In (a-d), zero lines are omitted.

References

Chen, P., M. P. Hoerling, and R. M. Dole, 2001: The origin of the subtropical anticyclones. *J. Atmos. Sci.*, **58**, 1827–1835.

Chou, C., J. D. Neelin, and H. Su, 2001: Ocean-atmosphere-land feedbacks in an idealized monsoon. *Quart. J. Roy. Meteor. Soc.*, **127**, 1869-1891.

Hoskins, B. J., 1996: On the existence and strength of the summer subtropical anticyclones. *Bull. Amer. Meteor. Soc.*, **77**, 1287-1292.

_____, and M. J. Rodwell, 1995: A model of the Asian summer monsoon. Part I: The global scale. *J. Atmos. Sci.*, **52**, 1329-1340.

_____, M.E. McIntyre and A.W. Robertson, 1985: On the use and significance of isentropic potential vorticity maps. *Quart. J. Roy. Met. Soc.,* **111**, 877-946.

Kalnay, E., M. Kanamitsu, and co-authors, 1996: The NCEP/NCAR 40-year reanalysis project. *Bull. Amer. Meteor. Soc.*, **77**, 437-471.

Kanamitsu, M.,W. Ebisuzaki, and co-authors,, 2002: NCEP-DOE AMIP-II Reanalysis (R-2). *Bull. Amer. Meteor. Soc.*, **83**, 1631-1643.

Klein, S. A., and D. L. Hartmann, 1993: The seasonal cycle of low stratiform clouds. *J. Climate*, **6**, 1587-1606.

Liu, Y., G. Wu, and R. Ren, 2004: Relationship between the subtropical anticyclones and diabatic heating. *J. Climate*, **17**, 682-698.

Ma, C.-C., C. R. Mechoso, A. Arakawa, and J. D. Farrara, 1994: Sensitivity of a coupled ocean-atmosphere model to physical parameterizations. *J. Climate*, **7**, 1883-1896.

Miyasaka, T., and H. Nakamura, 2004: Structure and formation mechanisms of the Northern Hemisphere summertime subtropical highs. Submitted to *J. Climate.*

Plumb, R. A., 1985: On the three-dimensional propagation of stationary waves. *J. Atmos. Sci.*, **43**, 217-229.

Rodwell, M. J., and B. J. Hoskins, 2001: Subtropical anticyclones and summer monsoons. *J. Climate*, **14**, 3192-3211.

Seager, R., R. Murtugudde, N. Naik, A. Clement, N. Gordon, and J. Miller, 2003: Air-sea interaction and the seasonal cycle of the subtropical anticyclones. *J. Climate*, **16**, 1948-1966.

Wang, Y., S.-P. Xie, B. Wang, and H. Xu, 2004: Large-scale atmospheric forcing by southeast Pacific boundary-layer clouds: A regional model study. *J. Atmos. Sci.* **61**, in press.

White, G. H., 1982: An observational study of the Northern Hemisphere extratropics summertime general circulation. *J. Atmos. Sci.*, **39**, 24-40.

Wu, G., and Y. Liu, 2003: Summertime quadruplet heating pattern in the subtropics and the associated atmospheric circulation. *Geophys. Res. Lett.*, **30 (5)**, 1201, doi:10.1029/2002 GL016209.